Supporting Information

Facile synthesis of flower-like $CePO_4$ with hierarchical structure for the simultaneous electrochemical detection of dopamine, uric acid and acetaminophen

Kai Zhu, Xinqin Cai, Yuhui Luo,* Botao Liu, Qingyu Zhang, Tongtong Hu, Zunzheng Liu, Haiying Wu, and Dongen Zhang*

Jiangsu Key Laboratory of Function Control Technology for Advanced Materials, School of Environmental and Chemical Engineering, Jiangsu Ocean University, Lianyungang 222005, Jiangsu province, China

* *Corresponding authors. E-mail: 2007000040@jou.edu.cn; luoyh@jou.edu.cn*

1. Materials

$Na_2HPO_4 \cdot 12H_2O$, $NaH_2PO_4 \cdot 2H_2O$, $NaH_2PO_2 \cdot H_2O$, urea, $Ce(NH_4)_2(NO_3)_6$ and KCl were purchased from Sinopharm Chemical Reagent Co., Ltd. UA, APAP, $K_3[Fe(CN)_6]$ and $K_4[Fe(CN)_6] \cdot 3H_2O$ were purchased from Aladdin Biochemical Technology Co., Ltd. 80% hydrazine hydrate was purchased from Hengxing Chemical Reagent Manufacturing Co., Ltd. DA was purchased from Macleans Biochemical Technology Co., Ltd. All reagents were of analytical grade and used without further purification.

2. Characterizations

The crystal structure of the sample was characterized by X-ray diffractometer (XRD; PANalytical, X'Pert PRO MPD). The diffractometer used Cu Kα (λ = 0.15406 nm) as the ray source. The working voltage and working current were 40 KV and 40 mA, respectively. The scanning range was $10\ ° \leq 2\theta \leq 70\ °$, and the scanning speed was 20 °/min. The Fourier Transform Infrared Spectroscopy (FTIR) was recorded on Nicolet-iS10. KBr was used for tableting, and the test range was 4000-400 cm^{-1}. X-ray photoelectron spectroscopy (XPS; Thermo Scientific K-Alpha) was used to obtain the elemental composition of the sample and the chemical state information of cerium. The Brunauer-Emmett-Teller (BET) surface area was obtained from the nitrogen adsorption-desorption isotherm under 77 K (BeiShiDe Instrument, 3H-2000PM1). Before the test, the sample was degassed at 150 °C for 180 min under vacuum. The surface charge information of the sample was characterized by a zeta potential analyzer (Malvern, Zetasizer Nano ZS90). The morphology and size of the sample were observed by scanning electron microscopy (SEM; JEOL, JSM-6390LA) and transmission electron microscopy (TEM; ZEISS, Libra 200FE).

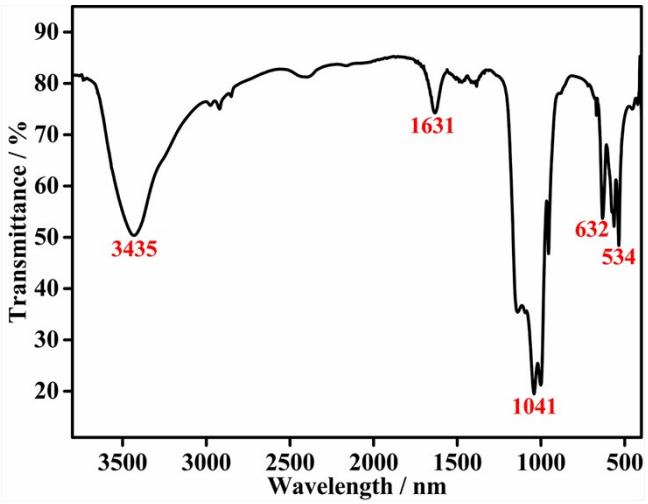

Fig. S1. FTIR spectrum of F-$CePO_4$.

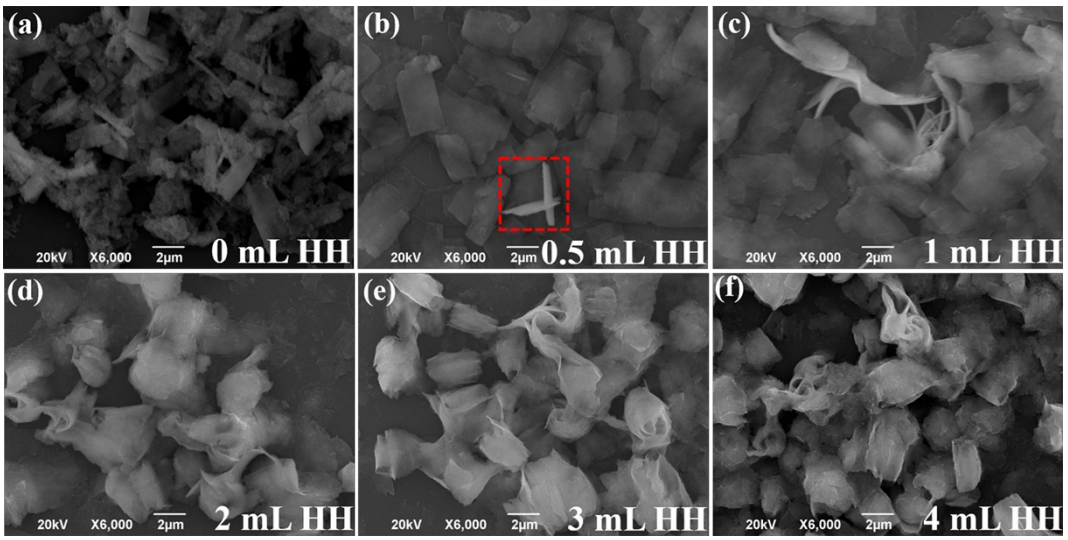

Fig. S2. SEM images of materials prepared with different amount of hydrazine hydrate.

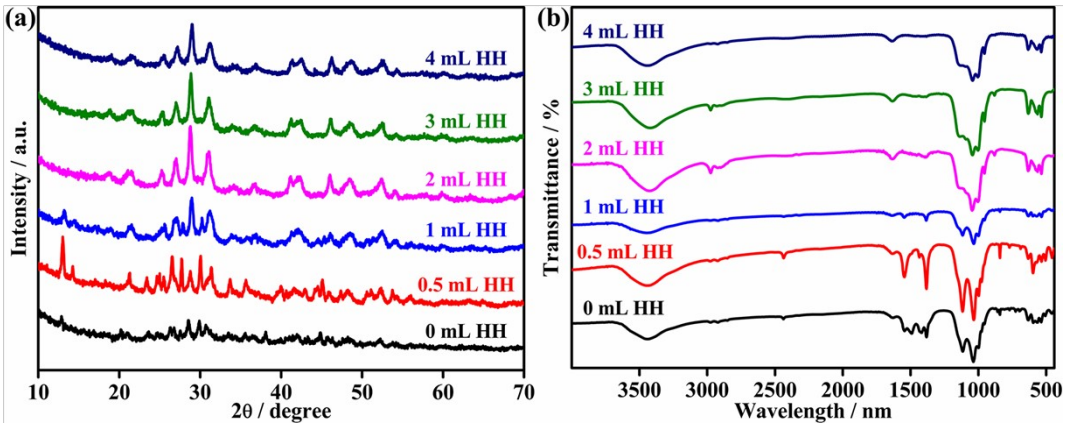

Fig. S3. XRD (a) and FTIR (b) spectra of materials prepared with different amounts of hydrazine hydrate.

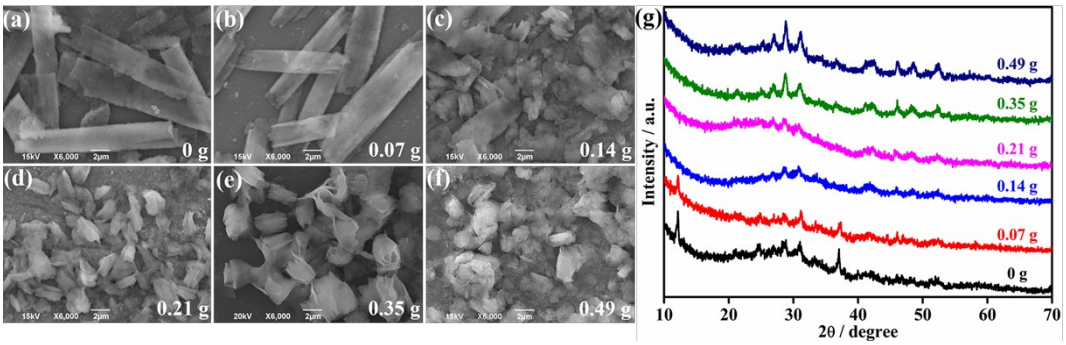

Fig. S4. SEM images and XRD patterns of the materials prepared with different amounts of urea.

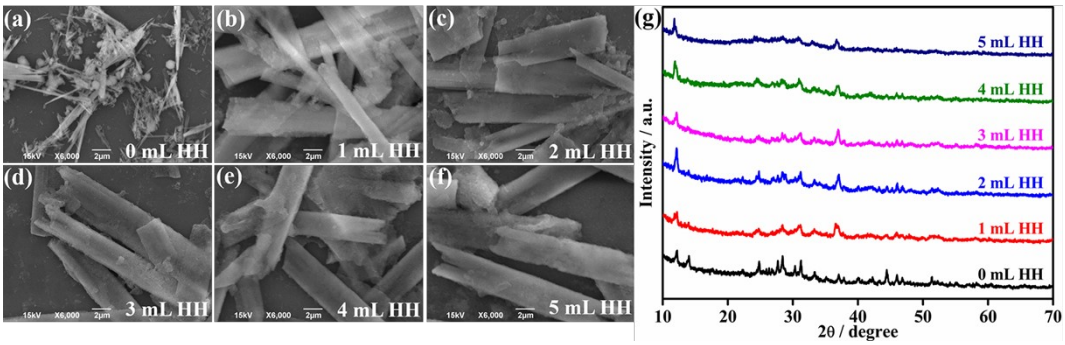

Fig. S5. SEM images and XRD patterns of the materials prepared by changing the amount of HH without adding urea.

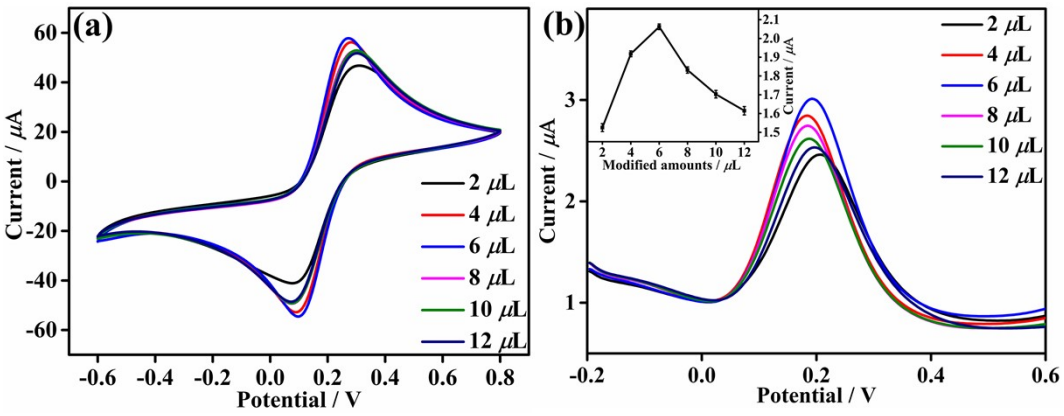

Fig. S6. (a) CV curves (100 mV/s) of GCE modified with different amounts of F-$CePO_4$ in 0.1 M KCl solution containing 5 mM $[Fe(CN)_6]^{3-/4-}$. (b) SWV curves of GCE modified with different amounts of F-$CePO_4$ in 0.1 M PBS (pH = 7.0) containing 150 μM DA. The inset is a line graph of peak currents and modified amounts.

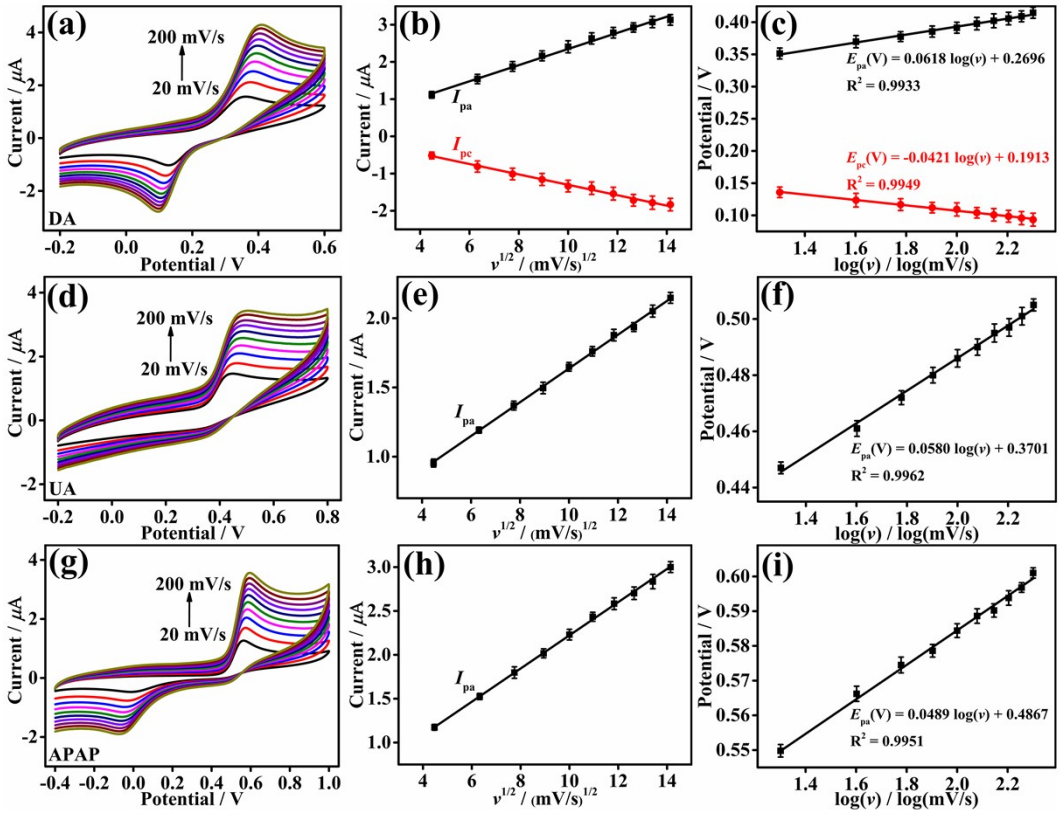

Fig. S7. CV curves of F-$CePO_4$ modified electrode at different scan rates (20-200 mV/s) in 0.1 M PBS (pH = 6.0) containing 100 μM DA (a), UA (d) and APAP (g). The linear fitting graphs of the peak current and the square root of the scan rate of DA (b), UA (e) and APAP (h). The linear fitting graphs of peak potential and log(v) of DA (c), UA (f) and APAP (i).

The number of electrons involved in the reaction (n) and the charge transfer coefficient (α) can be calculated using the following equations [1-3].

$$E_{pa} = E^{\theta} + 2.3RT/((1 - \alpha)nF)\log(v) \quad (1)$$

$$E_{pc} = E^{\theta} - 2.3RT/(\alpha nF)\log(v) \quad (2)$$

$$E_p = E^{\theta} + 2.3RT/(\alpha nF)\log(K^{\theta}RT/(\alpha nF)) + 2.3RT/(\alpha nF)\log(v) \quad (3)$$

In equations (1) - (3), E^{θ} is the formal redox potential, K^{θ} is the standard rate constant of the reaction, F is the Faraday constant (96485 C/mol), and v is the scan rate. As the scan rate increases, there is also a good linear relationship between the peak potential and log(v) of DA. As shown in Fig. S7c, the linear equations are E_{pa}(V) = 0.0618log(v) + 0.2696 (R^2 = 0.9933) and E_{pc}(V) = -0.0421log(v) + 0.1913 (R^2 = 0.9949). Combining equations (1) and (2), the n and α values of DA can be calculated as 2.36 and 0.59. The electrode reaction processes of UA and APAP are irreversible, and α can be estimated as 0.5. As shown in Fig. S7f and S7i, the linear relationship

between the peak potential and log(v) of UA and APAP are E_{pa}(V) = 0.0580log(v) + 0.3701 (R^2 = 0.9962) and E_{pa}(V) = 0.0489log(v) + 0.4867 (R^2 = 0.9951). Combining equation (3), it can be calculated that n of UA and APAP are 2.04 and 2.42, respectively. This means that the number of electrons involved in the electrode reaction is 2. This is consistent with previous reports [4,5]. Therefore, the possible redox processes of DA, UA and APAP can be proposed, as shown in Fig. S8 [6].

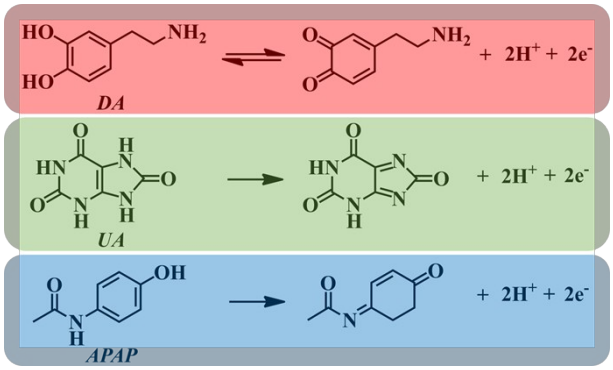

Fig. S8. Electrochemical reaction mechanism of DA, UA and APAP.

Table S1. The detection limits and linear ranges of DA, UA and APAP with different modified electrodes.

Electrode material	Detection limit / μM			Linear range / μM			References
	DA	UA	APAP	DA	UA	APAP	
g-C_3N_4/Co	0.4	—	—	2.0–400	—	—	ChemElectroChem 7 (2020) 1373-1377
GO/$TmPO_4$	0.78	—	—	2–20	—	—	Microchem. J. 160 (2021) 105694
TiO_2/RGO	6	—	—	2–60	—	—	Sci. Rep. 4 (2014) 5044
Graphene/SnO_2	3	—	—	1–20	—	—	J. Electroanal. Chem. 749 (2015) 26-30
Au-SiO_2	1.98	—	—	10–100	—	—	Surf. Interfaces 14 (2019) 82-91
HNP-PtTi	3.2	5.3	—	4–500	100–1000	—	Biosens. Bioelectron. 82 (2016) 119-126
GO/MWNT	1.5	1	—	5.0–500	3.0–60	—	Biosens. Bioelectron. 56 (2014) 300-306
RGO-Ag/PANI	0.2	0.2	—	5–200	20–350	—	Chem. Res. Chinese U. 33 (2017) 507-512
Au/RGO	—	1.8	—	—	8.8–530	—	Sensor. Actuat. B-Chem. 204 (2014) 302-309
MoS_2/PEDOT	—	0.95	—	—	2–25	—	Microchim. Acta 183 (2016) 2517-2523
ERG	—	—	1.2	—	—	5-800	Electrochim. Acta 162 (2015) 198-204
PEDOT/GO	—	—	0.57	—	—	10-60	Sensor. Actuat. B-Chem. 193 (2014) 823-829
MWCNT/PE	—	—	0.57	—	—	5-92.6	J. Electroanal. Chem. 696 (2013) 52-58
MWCNT-PDDA-PSS/GE	—	—	0.5	—	—	25-400	Electrochim. Acta 56 (2011) 6619-6627
AuNP-PGA-SWCNT	—	—	1.18	—	—	8.3-145	Sensor. Actuat. B-Chem. 174 (2012) 318-

							324
F-$CePO_4$	0.17	0.38	0.13	2.0-1130	2.5-835	1.0-900	This work

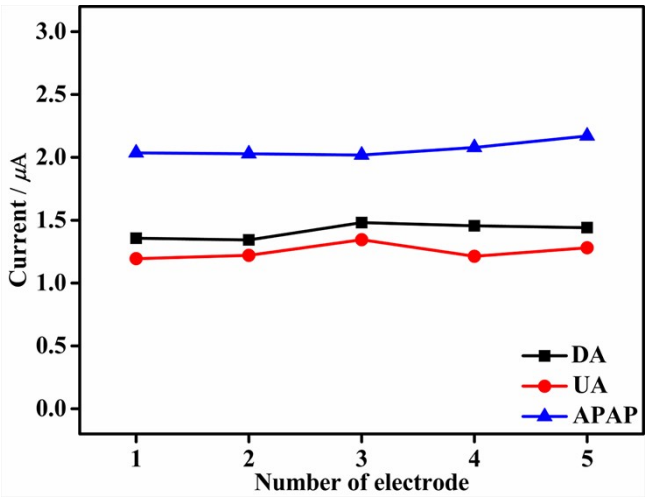

Fig. S9. The peak current of different F-$CePO_4$@GCE in 0.1 M PBS (pH = 6.0) containing 100 μM DA, UA and APAP.

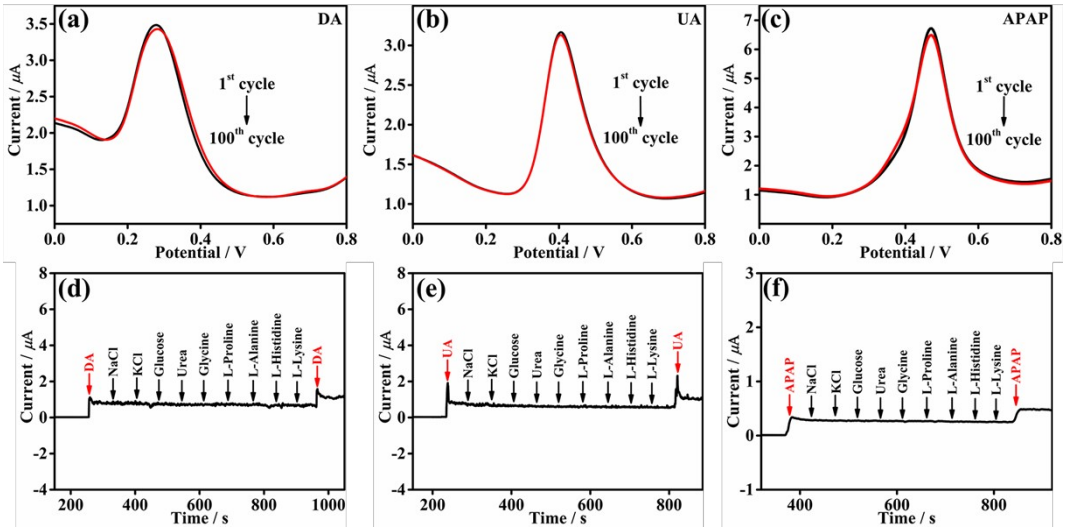

Fig. S10. The SWV curve of the first circle and the 100th circle in 0.1 M PBS (pH = 6.0) containing 150 μM DA (a), UA (b) and APAP (c) respectively. (d-f) Current response of F-$CePO_4$@GCE to the detection substance and 20 times concentration of interfering substance in 0.1 M PBS (pH = 6.0) (Potential is 0.45V).

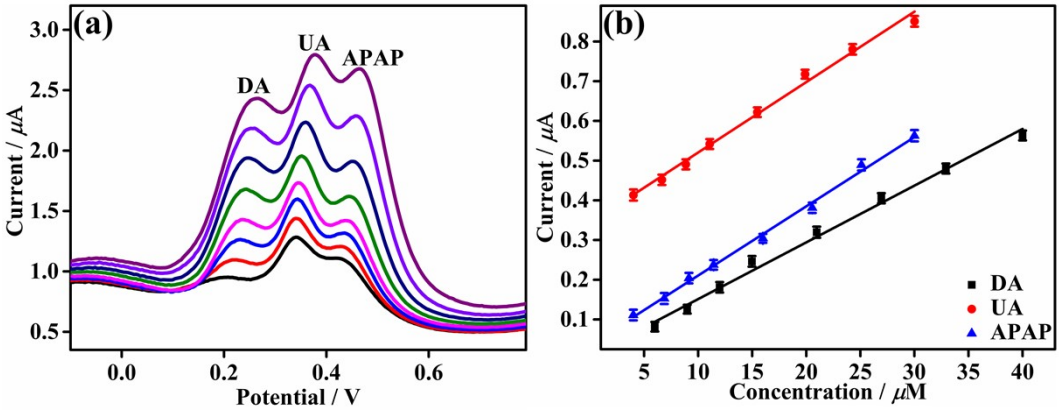

Fig. S11. (a) SWV curves of F-$CePO_4$@GCE in 0.1 M PBS (pH = 6.0) with different concentrations of DA, UA and APAP. (b) Linear fitting of peak current and concentration of DA, UA and APAP.

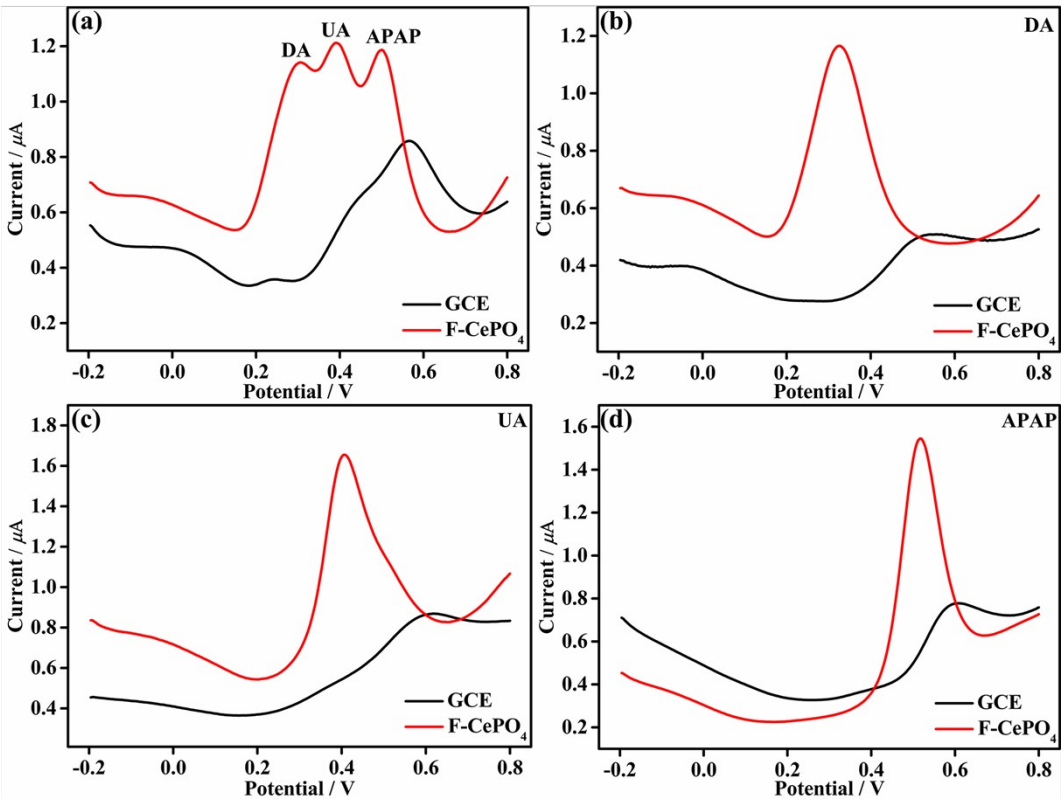

Fig. S12. (a) SWV curves of F-$CePO_4$ modified electrode and bare electrode in 0.1 M PBS (pH = 6.0) containing DA, UA and APAP. (b-d) SWV curves of F-$CePO_4$ modified electrode and bare electrode in 0.1 M PBS (pH = 6.0) containing 50 μM DA, UA and APAP respectively.

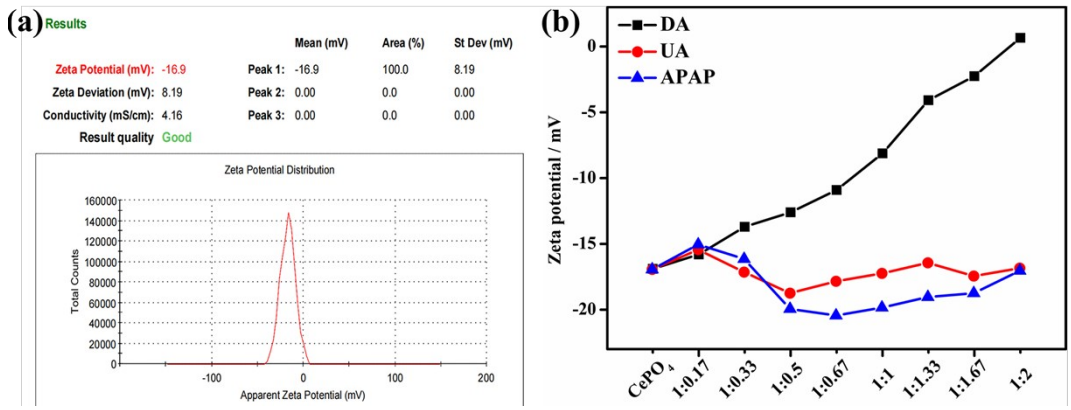

Fig. S13. (a) The zeta potential of F-$CePO_4$ suspension. (b) The zeta potential relationship diagram of F-$CePO_4$ suspension mixed with DA, UA and APAP aqueous solutions in different volume ratios.

References

[1] E. Laviron, *J. Electroanal. Chem. Interfacial Electrochem.*, 1979, **101**, 19-28.

[2] Y. Dang, Y. Zhai, L. Yang, Z. Peng, N. Cheng and Y. Zhou, *RSC Adv.*, 2016, **6**, 83994-84002.

[3] N.C. Honakeri, S.J. Malode, R.M. Kulkarni and N.P. Shetti, *Sensors International*, 2020, 1, 100002.

[4] S. Immanuel, T.K. Aparna and R. Sivasubramanian, *Surf. Interfaces*, 2019, **14**, 82-91.

[5] A. Cernat, M. Tertis, R. Sandulescu, F. Bedioui, A. Cristea and C. Cristea, *Anal. Chim. Acta*, 2015, **886**, 16-28.

[6] T. Iranmanesh, M.M. Foroughi, S. Jahani, M.S. Zandi and H.H. Nadiki, *Talanta*, 2020, **207**, 120318.